Quarterly Journal of Engineering Geology and Hydrogeology

Petrophysical and durability tests on sedimentary stones to evaluate their quality as building materials

G. Cultrone, A. Luque and E. Sebastián

Quarterly Journal of Engineering Geology and Hydrogeology 2012, v.45; p415-422.
doi: 10.1144/qjegh2012-007

Notes

Petrophysical and durability tests on sedimentary stones to evaluate their quality as building materials

G. Cultrone*, A. Luque & E. Sebastián

Department of Mineralogy and Petrology, Faculty of Sciences, University of Granada, Granada, Spain
*Corresponding author (e-mail: cultrone@ugr.es)

Abstract: Six types of sedimentary stone (four bioclastic calcarenites, one calcitic sandstone and one calcitic dolostone) commonly used as building materials were studied from a petrophysical point of view and their durability was evaluated. The following analytical techniques were used: X-ray diffraction, polarizing optical microscopy, hydric tests, mercury intrusion porosimetry, ultrasound, salt crystallization cycles, freeze–thaw cycles and colorimetry. The hydric behaviour of the stones is affected by their different textures. The most compact stone absorbs less water compared with the other samples and has the lowest open porosity; however, more porous and less compact stones achieved better results in terms of the degree of pore interconnection and the drying rate. All the stones have unimodal pore size distribution and most pores had radii of 10 μm or less. Accelerated ageing tests caused some changes in the colour of stones and, above all, the loss of fragments, especially during salt crystallization cycles. The main causes of decay were the different mineralogy between the grains and the matrix in the sandstone and a strong anisotropy owing to the presence of sedimentary planes in one calcarenite. On the basis of our results we then ranked the stones according to their quality as building materials.

Natural stone has been used in both building and artwork since ancient times and it continues to be highly regarded (Fort 2008). Among the wide range of stones used for these purposes, marbles and granites are highly prized for their use in important monuments and sculptures and because their surfaces can be polished, so enhancing their appearance. However, a large part of our architectural heritage is composed of sedimentary stones with rough surfaces and visible porosity. The look and characteristics of sedimentary stones depend on their mineralogical composition, and the depositional environment and diagenesis to which the sediments were subject. By studying the petrophysical features of these stones we can establish their quality as building and/or ornamental materials. For this purpose, the choice of one stone over another depends, above all, on its physical rather than its aesthetic properties, as building materials must be able to withstand exposure to the weather, pollution and other decay agents. Durability (or its opposite, deterioration) is a complex and crucial factor to be considered when choosing building stone. Stone deterioration is a common, irreversible phenomenon (Kühnel 2002), with continuous effects that vary depending on the composition and texture of stone and the environment in which it is located (Charola 2004). Physical, chemical and biological processes all play a part and interact in the stone deterioration process (Veniale *et al*. 2008). By using a series of analytical techniques we can find out more about the quality of a stone and detect its weak points with respect to particular decay agents (Török & Prikryl 2010; Anania *et al*. 2012).

The aim of this work is to study the petrophysical characteristics of a selected group of sedimentary stones used as construction materials, to evaluate their durability and to establish a ranking order on the basis of their quality.

The most commonly used sedimentary stones in our architectural heritage are sandstones and limestones, which can be seen in many monuments in our historical city centres as well as in new buildings (Ashurst & Dimes 1990). Pure calcitic limestone has been shown to be less resistant than pure silicic sandstone, and, in general, stones in which the matrix has a different composition from that of its clasts will be less resistant to decay (Charola 2004). However, in addition to their mineralogy, the durability of these stones also depends on their compactness and their pore system, within which water and soluble salts can circulate, so causing decay (Anselmetti *et al*. 1998; Hall & Hoff 2002; Alves *et al*. 2011). In this work we will therefore also be studying the parameters of porosity and pore size distribution and combining the results.

Materials and methods

Six sedimentary stones were investigated, all of them currently quarried in the province of Jaen (Spain) and on sale as construction materials (Fig. 1): one comes from the Bujalance area (J1), two from Baeza (J2 and J3), one from Sabiote (J4) and two from Cazorla (J5 and J6). They have been supplied by local stone industries.

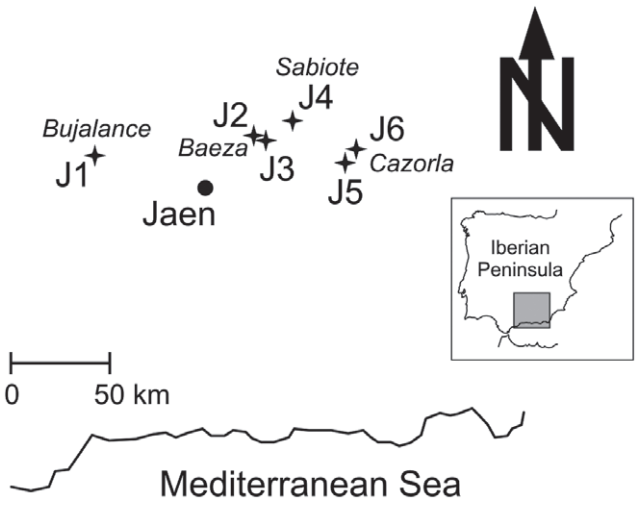

Fig. 1. Geographical location of the stones quarried in the province of Jaen (southern Spain): J1 from Bujalance; J2 and J3 from Baeza; J4 from Sabiote; J5 and J6 from Cazorla.

Quarterly Journal of Engineering Geology and Hydrogeology, **45**, 415–422
DOI: 10.1144/qjegh2012-007.

Table 1. *Mineral phases (in %) of the stones from Bujalance (J1), Baeza (J2 and J3), Sabiote (J4) and Cazorla (J5 and J6) determined by XRD analysis*

	Cal	Dol	Qz	Fsp	Ms	Chl
J1	42	2	41	1	12	2
J2	68	16	13	3		
J3	64	13	21	2		
J4	34	63	3			
J5	84		16		1	
J6	81	11	8			

Cal, calcite; Dol, dolomite; Qz, quartz, Fsp, feldspars (in general); Ms, muscovite; Chl, chlorite. Mineral abbreviations after Whitney & Evans (2010).

The mineralogy of the six stones was studied by X-ray diffraction (XRD) using a Philips PW-1710 diffractometer with graphite monochromator, automatic slit, Cu*K*α radiation (λ = 1.5405 Å), at 40 kV and 40 mA. The data were collected in continuous scanning mode with 0.02° goniometer rate and 2θ from 3 to 60°. XRD goniometric calibration was performed using a silicon standard. Samples were milled in agate mortar to <40 μm particle size and then analysed. The resulting data were interpreted using XPowder software (Martín 2004).

The mineralogy and texture of the samples were assessed using a polarizing optical microscope (Zeiss Jenapol). A third of each section was stained red with alizarin to distinguish calcite from dolomite (which does not stain) and then observed with parallel and crossed Nicols.

The parameters associated with fluid transport inside the pores were determined by hydric tests. The results of free and forced (under vacuum) water absorption (EN13755, Anonymous 2008), and drying tests (NORMAL 29/88, Anonymous 1988) were determined by weighing the samples (three samples per stone type) at regular intervals. Samples were cut into cubes with a 5 cm edge. The drying rate, the real (skeletal) and apparent density, the open porosity (RILEM 1980) and the degree of pore interconnection (Molina *et al*. 2011) were calculated. This last parameter offers an insight into the tortuosity of the pore system of the stones and was measured by comparing free and forced water absorption values. Because many weathering processes depend on water circulation inside the stone, this parameter is extremely important in the evaluation of durability (Cultrone *et al*. 2003).

The distribution of the pore access size as well as the pore volume of the stones was determined using a Micromeritics Autopore III 9410 porosimeter (MIP), which can measure pores with diameters between *c*. 0.003 and 360 μm. Freshly cut samples chips of *c*. 2 cm^3 were oven dried for 24 h at 110 °C and then analysed. Two MIP measurements per sample were made.

Ultrasound measurements were performed to evaluate the degree of compactness of the six types of stone, as ultrasonic waves are directly influenced by the petrological features of stone such as pores, grain sizes and composition (García del Cura *et al*. 2005). The measurements were performed on 5 cm edge cubes (three cubes for each stone type) using a Panametrics HV Pulser/Receiver 5058PR coupled with a Tektronix TDS 3012B oscilloscope. The propagation velocity of compressional (V_P) and shear (V_S) pulses was measured in accordance with the ASTM D 2845 standard (ASTM 1983) for dry test samples using polarized Panametrics transducers of 1 GHz. A viscoelastic couplant was used to ensure good coupling between transducers and stone cubes. The velocity of the ultrasound waves was determined under controlled thermohygrometric conditions (25 °C and relative humidity 50%). Poisson's ratio, Young's modulus, shear and bulk modulus (Cultrone & Sebastián 2009), and the indices for total and relative anisotropy (Guydader & Denis 1986) were also calculated.

We concluded our experiments by subjecting the stones to salt crystallization and freeze–thaw tests to evaluate their durability. In accordance with the EN 12370 standard (Anonymous 2001), we carried out 15 salt crystallization cycles of 24 h each using a solution of 14% $NaSO_4.10H_2O$. The transition from an anhydrous to a decahydrate phase causes an increase of 314% in volume (Winkler 1997). This test provided information on the damaging effects of soluble salts that are usually present in water and can crystallize inside pores and fissures. One of the most dangerous of the salts detected in historical buildings is sodium sulphate because of its strong crystallization pressure when it precipitates in porous media from a supersaturated solution (Ruiz Agudo *et al*. 2006). Moreover, 30 freeze–thaw cycles of 24 h each were performed according to the EN 12371 standard (Anonymous 2003) to evaluate how the texture and pore system were affected by water changing from a liquid to a solid state. In both tests, we used three 5 cm edge cube-shaped samples per stone and damage was assessed by a visual inspection of material loss and by measuring weight changes. In addition, the overall colour change (Δ*E*) in the stones produced by these ageing tests was quantified using a portable Minolta CM700d spectrophotometer. The chromatic coordinates (*a** and *b**) and lightness (*L**) were measured using an illuminated area of 8 mm in diameter. We used a CIE D65 illuminant, which simulates daylight with a colour temperature of 6504 K.

Results and discussion

Mineralogy and texture

Of the stones analysed in this study, J1 is the only one with more siliciclastic components than carbonates (Table 1). It is a calcitic sandstone of Messinian age that crops out to the west of Jaen near Porcuna, where it was used in various historical monuments (IGME 1975). The silicilastic components are mainly composed of angular-shaped quartz grains characterized by undulose extinction, which suggests a metamorphic origin (Fig. 2a). Muscovite has been identified by XRD and observed under optical microscopy with its typical laminar habit. There are sporadic chlorite laminae and plagioclase grains with polysynthetic twinning. Both the matrix and the few fossil fragments in the stone are formed by carbonates. The carbonates join the siliciclastic particles together and are composed almost exclusively of calcite, with very low dolomite abundance. This stone has interparticle porosity and irregular-shaped pores of similar size.

J2 and J3 are two stone varieties from the same calcarenitic formation of Serravallian age. They have different degrees of cementation, which means that for commercial purposes J2 is classified as 'Piedra Franca' (weak stone) and J3 as 'Piedra Viva' (hard stone). These stones have been used widely in the architectural heritage of Baeza (Sebastian Pardo *et al*. 1995; Alcalde *et al*. 1998), a UNESCO World Heritage Site to the north of Jaen. Both stones are yellow–cream coloured and mainly composed of fossil fragments of calcitic composition (bryozoans, corals, bivalves and echinoderms) (Fig. 2b). They are therefore classified as bioclastic calcarenites. Calcite represents more than 60% of the mineral content (Table 1), and is slightly more abundant in the 'Franca' variety. A smaller percentage of dolomite was detected. The matrix is composed of both micritic and sparitic carbonates (sometimes with polysynthetic twinning), although there is more sparitic material in the 'Viva' variety (Fig. 2c). The siliciclastic component consists mainly of angular to subrounded quartz grains of metamorphic origin. Rare feldspathic grains were also identified. The pores in J3 are irregular in shape, whereas in J2 they are somewhat larger and elongated to rounded. Porosity is mainly intergranular although some intragranular pores are visible within fossils.

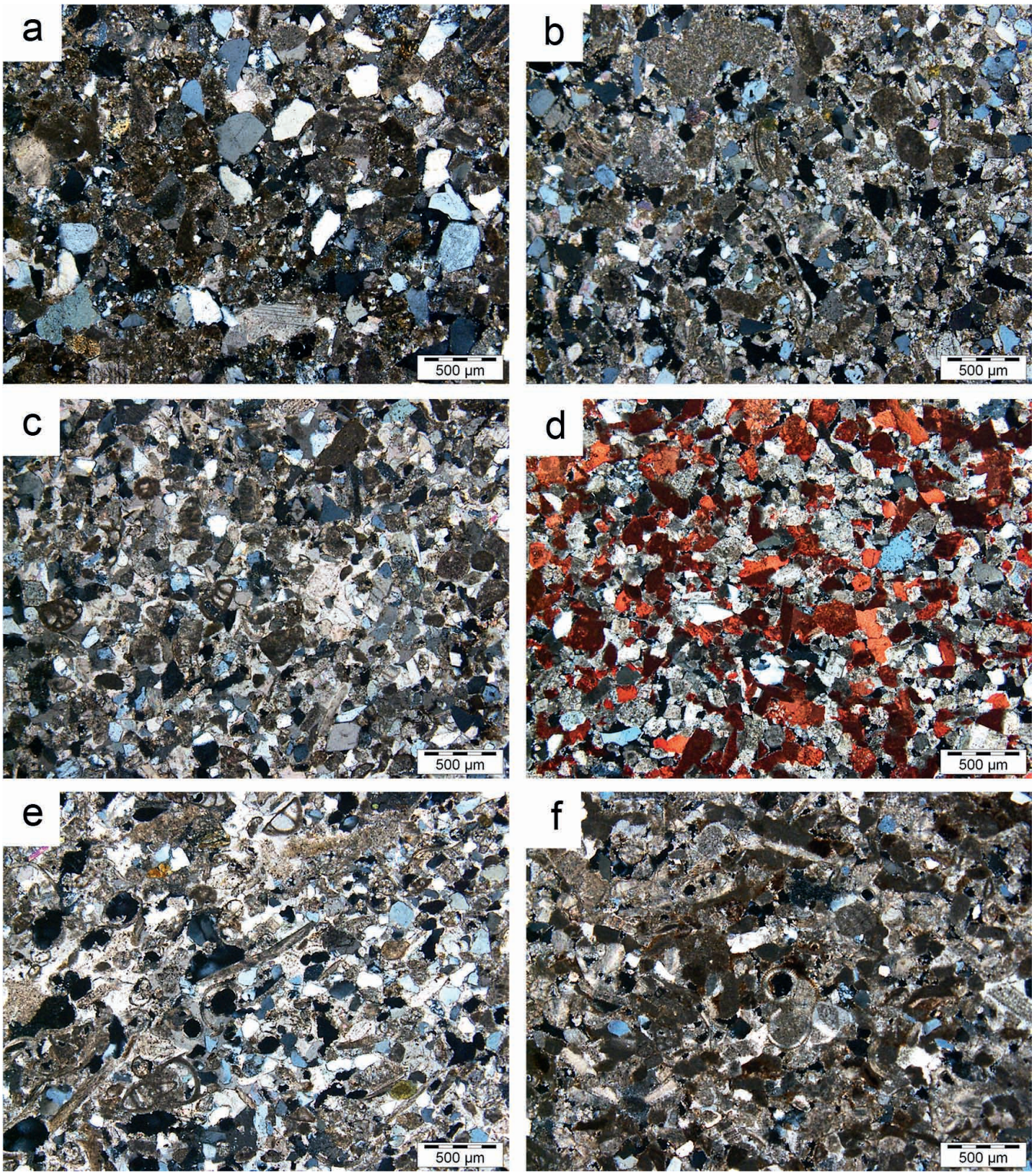

Fig. 2. Optical microscopy images: (**a**) calcitic sandstone from Bujalance (J1); (**b**) bioclastic calcarenite 'Piedra Franca' from Baeza (J2); (**c**) bioclastic calcarenite 'Piedra Viva' from Baeza (J3); (**d**) calcitic dolostone from Sabiote (J4); (**e**) bioclastic calcarenite from Cazorla (J5); (**f**) bioclastic calcarenite from Cazorla (J6).

A notable feature of J4 is its high dolomite content (Fig. 2d), which is higher than that of calcite (Table 1). This is a calcitic dolostone of Early Jurassic age that crops out to the north of Baeza. Carbonate grains usually show cleavage planes, whereas polysynthetic twins have been observed only in calcite grains. The matrix is both sparitic and micritic, and the micrite is composed exclusively of calcite. Quartz grains are rare, characterized by undulose extinction and generally smaller than the carbonate grains. Porosity is interparticle.

J5 and J6 have been used occasionally as building materials in the Cazorla area and are classified as bioclastic Serravallian calcarenites. J5 is characterized by a nearly planar lamination in which yellowish beds 2–4 mm thick alternate with darker planes. It is the only stone in which carbonates are exclusively represented by

calcite (Table 1) and are made up of fragments of fossils (echinoderms, bryozoans and algae). Angular to subrounded quartz fragments of metamorphic origin are also visible. Traces of phyllosilicates were identified by XRD and observed under optical microscopy (Fig. 2e). These laminar crystals were responsible for the lamination visible to the naked eye. Pores have irregular shapes and sizes and are both inter- and intraparticle.

J6 is more than 90% carbonates (Table 1), which are mainly composed of calcitic fossil fragments. Dispersed dolomite grains and angular to subrounded quartz fragments can also be distinguished. Grains are cemented by micritic and sparitic carbonates. The sparite usually shows polysynthetic twins and the typical rhombohedral cleavage. Pores are both intragranular (inside the fossils) and intergranular (among the grains) and of variable size. Red to brown Fe oxides pigment the matrix along the edges of the pores and between the grain boundaries (Fig. 2f), and are responsible for the reddish colour of the stone.

Pore system

The MIP technique provides clear information about the pore system of the stones and completes the observation carried out under the microscope. All samples show unimodal distribution suggesting a homogeneous pore size even when a second family of pores is detected, as occurred in the two stones from Cazorla (J5 and J6, Fig. 3). The main peak for pore size was situated at around 10 μm except in J3 and J6, in which the maximum was at 2.6 and 4.2 μm, respectively. The lowest porosity accessible to Hg (p_{oMIP}, Fig. 3) was measured in J3 (8.08%), whereas the highest was in J6 (21.51%). The other stones show intermediate values.

The open porosity and the pore size influence the circulation of water inside the stones. J6 is the stone with the highest free and forced water absorption levels (see Fig 4 and A_b and A_f values in Table 2). At the opposite end of the scale, J3 stands out for its very low absorption capability (A_b = 2.52% and A_f = 3.33%). The other four stones show intermediate values. The degree of pore interconnection (Ax) is highest in J3 (24%), confirming that it is difficult for water to flow inside the stone. However, the difference from the other stones is not very marked. Only J5 shows a better connectivity between pores, which is probably due to its particular texture (planar lamination). Another characteristic feature of this stone is that it has the highest saturation coefficient value (S, Table 2). This parameter is clearly linked to Ax; in fact, the easier the movement of water inside the stone (low Ax values), the higher the S value. All samples start drying quickly and the slopes of the drying curves are parallel to each other (Fig. 4). In this first phase of drying the pore structure of the stones has no significant influence on the drying rate, which is constant ('constant rate period'; Scherer 1990). The drying rate changes when 'critical moisture content' is reached (Kirk & Othmer 2004) and water loss now depends on the movement of water vapour from the pores to the surface ('falling rate period'; Scherer 1990). In this second phase, drying depends on the type of pores and the degree of interconnection, and useful information can be gained by comparing the drying index values (Di, Table 2). Given that water is always involved in stone decay processes (Charola 2004), low Di values may be a sign of more durable materials (Molina *et al*. 2011). The stones with the highest Di values, J3 (Di = 1.15) and J4 (Di = 1.16), therefore dry slowly and may decay more easily (Table 2). The difficulty that J3 and J4 have in drying is also confirmed by the fact that they had the highest Ax values (24% and 23.47%, respectively). The other samples dried slightly more quickly and at almost the same rate. The open porosity (p_o, Table 2) showed similar values to those measured by MIP (p_{oMIP}, Fig. 3), especially when we compared the stones with the highest and lowest p_o values. The small differences compared with the other stones can be attributed to the differences between the two techniques (mainly, the use of two fluids, i.e. mercury and water, and the intrusion pressures exerted). The real density values calculated (ρ_{sk}, Table 2) are compatible with the mineralogy of the stones previously determined by XRD. In fact, the lowest value was calculated in J1, which is the stone with the highest quartz content (ρ_{qtz} = 2.66 g cm^{-3}), whereas the densest rock was J4, which is mainly composed of dolomite, the densest mineral component of the stones we studied (ρ_{dol} = 2.88 g cm^{-3}).

Compactness

Ultrasonic velocity tests showed that the dynamic behaviour of the six stones varies in line with their mineralogy, texture, density and porosity (Table 3).The highest V_P and V_S values were measured in J3 (3571 m s^{-1} and 2120 m s^{-1}, respectively), which suggests that this is the most compact of the studied stones (as well as the least porous; see Table 2). The lowest velocity values were for J2, in which V_P values are *c*. 20% less than those of J3. In these two stones, which are from the same geological formation and have almost identical mineralogy (i.e. the 'weak' and 'hard' stones from Baeza), porosity is the main factor influencing the velocity values (see Table 2).

As regards anisotropy, the stone with the highest ΔM and Δm values is J5 (10.83% and 17.73%, respectively), which is the only stone in which sedimentary beds were observed. At the opposite end of the scale are J4 (3.65% and 1.33%) and J6 (2.87% and 3.93%); this result suggests that the texture of these two stones is homogeneous (Table 3).

The mineralogy of the stones, and in particular their calcite content (see Table 1), directly influences the Poisson's ratio (ν; Domenico 1983; Ji *et al*. 2009). In fact, J5, which is the richest stone in calcite, shows the highest ν value (0.31), whereas the lowest values were for J1 and J4 (0.23 and 0.22, respectively), the poorest in this phase. The shear modulus (G) and Young's modulus (E) provide similar results, with the highest values being measured in J3 (G = 17.26 MPa and E = 6.80 MPa). The other stones show similar values, with the lowest results being obtained for J2 (G = 9.98 MPa and E = 3.87 MPa). As regards the bulk modulus (K), the highest compressive resistance was for J5 (12.64 MPa), followed closely by J3 (12.53 MPa), whereas the weakest stone appears to be J1 (6.87 MPa, Table 3).

Durability

The salt crystallization test had a considerable effect on the stability of the samples, causing the rounding of most sample edges and in some cases the development of cracks. All samples showed an initial weight increase owing to the presence of salt crystals in the pore system of stones, and J6 was the one that increased most (Fig. 5a), owing to its high porosity and water absorption values (p_o, A_b and A_f values, Table 2). However, the weight of J6 remained fairly constant and by the end of the test it had undergone only minimal weight loss (1.73%) because of sanding of some edges (Table 4). This was the second best result, bettered only by J3, the curve for which remained close to zero throughout the 15 test cycles (Fig. 5a). Its weight loss was negligible (0.22%) and no visual damage was observed. J1 and J5, on the other hand, showed severe loss of material (23.98% and 22.67%, respectively; see Table 4). J1 was the first stone that started to break up, after six cycles, and small fragments continued breaking off until the end of the test. J5 behaved similarly to the other samples until the 13th cycle, when it broke along its marked sedimentary planes. J2 and J4 showed intermediate results nearer those of the stones with good

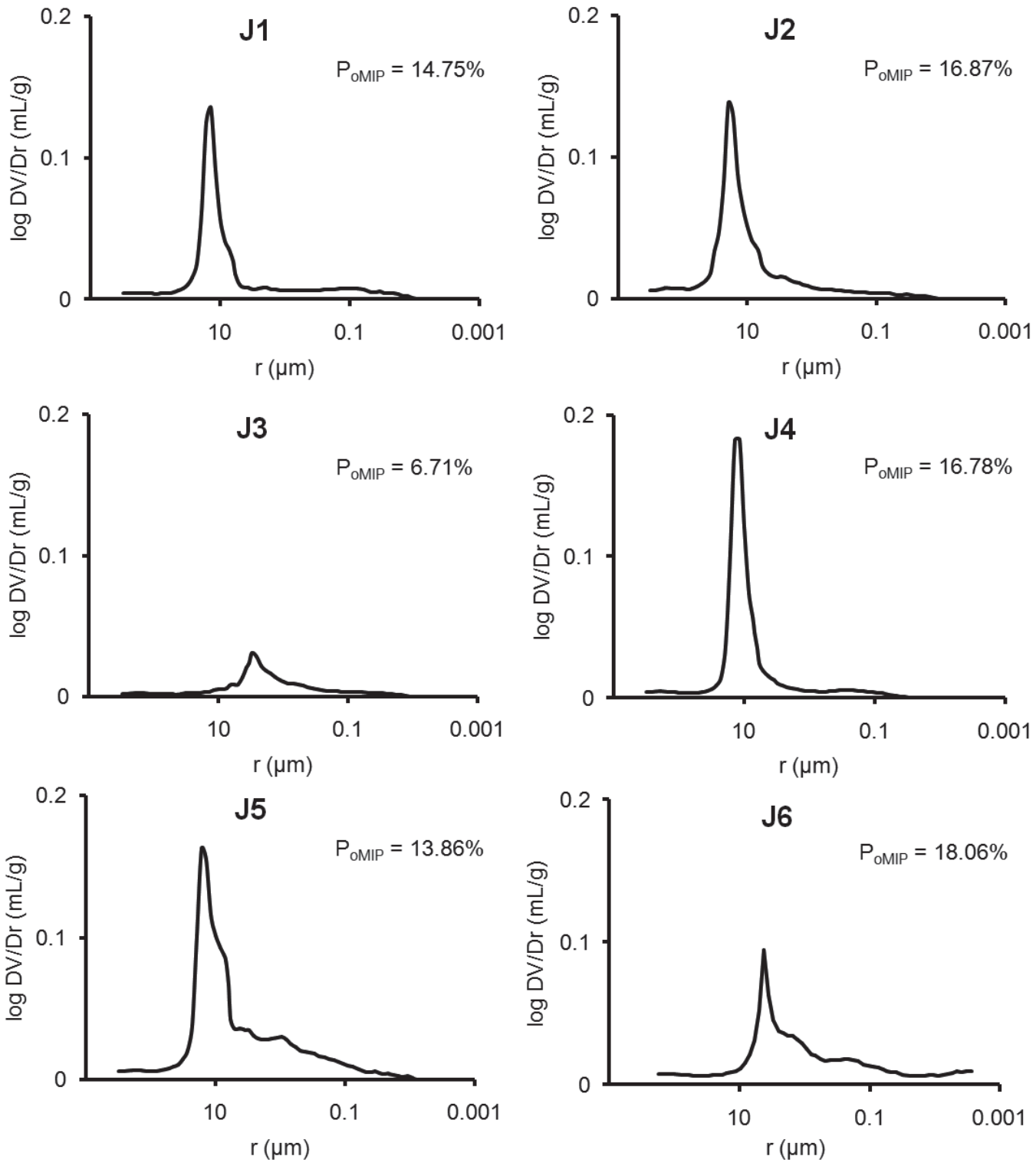

Fig. 3. MIP pore size distribution curves (i.e. log differential intruded volume (ml g^{-1}) v. pore radius (mm)) of the stones from Bujalance (J1), Baeza (J2 and J3), Sabiote (J4) and Cazorla (J5 and J6). Open porosity (p_{oMIP}) value of each stone is indicated.

behaviour. Only partial sanding of edges was observed. If we take into account the similarity in the pore size distribution of J1 and J5 to those of other stones that performed better (i.e. J2 and J4, Fig. 2), their poor results may be due to their texture; that is, the differing composition between grains and matrix in J1, which confirms that this stone is less durable than those in which grains and matrix have the same composition (Charola 2004), and the marked anisotropy in J5, which was observed by the naked eye and confirmed by ultrasound (Table 3). This anisotropy favours a higher physical deterioration along preferred planes compared with stones with similar composition but a more isotropic texture (Sebastián *et al*. 2008).

There are clear differences in the response of the stones to the freeze–thaw test (Fig. 5b) when compared with that to salt crystallization. In general, the stones were more resistant to decay and the only change detected during the test was a weight increase owing

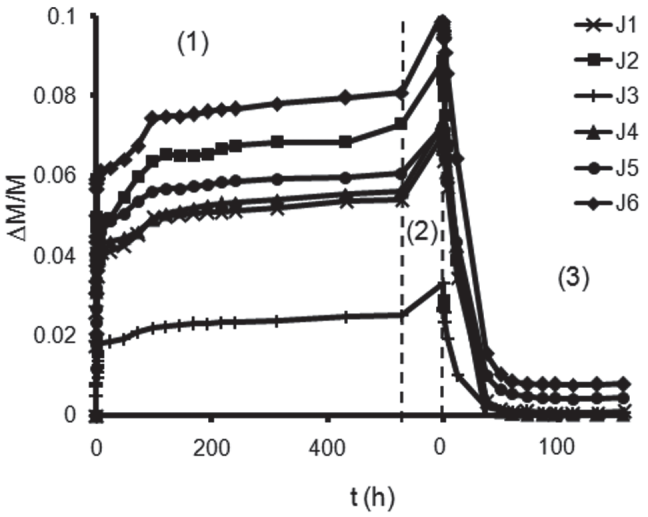

Fig. 4. Free water absorption (1), forced saturation (2) and drying (3) of the stones from Bujalance (J1), Baeza (J2 and J3), Sabiote (J4) and Cazorla (J5 and J6). Weight variation ($\Delta M/M$) v. time (in hours).

Table 2. *Hydric parameters for the stones from Bujalance (J1), Baeza (J2 and J3), Sabiote (J4) and Cazorla (J5 and J6)*

	J1	J2	J3	J4	J5	J6
A_b	5.41	7.29	2.52	5.60	6.06	8.09
A_f	7.05	8.88	3.33	7.32	7.24	10.13
Ax	23.18	17.95	24.00	23.47	14.18	20.36
S	60.54	61.45	58.31	60.73	73.29	63.06
Di	0.97	0.96	1.16	1.15	0.97	0.95
p_o	14.15	18.94	8.08	16.77	15.55	21.51
ρ_b	2.00	2.13	2.43	2.29	2.21	2.13
ρ_{sk}	2.34	2.63	2.64	2.75	2.61	2.71

A_b, free water absorption (%); A_f, forced water absorption (%); *Ax*, degree of pore interconnection (%); *S*, saturation coefficient (%); *Di*, drying index; p_o, open porosity (%); ρ_b, apparent density (kg m^{-3}); ρ_{sk}, real (skeletal) density (kg m^{-3}).

Table 3. *Average velocities for the propagation of ultrasonic V_P and V_S pulses (m s^{-1}) for the stones from Bujalance (J1), Baeza (J2 and J3), Sabiote (J4) and Cazorla (J5 and J6)*

	J1	J2	J3	J4	J5	J6
V_P	3571	3493	4212	3704	4171	3562
V_S	2120	1906	2364	2210	2120	1994
ΔM	5.22	8.26	6.00	3.65	10.83	2.87
Δm	5.67	7.90	4.94	1.33	17.73	3.93
ν	0.23	0.29	0.27	0.22	0.31	0.27
E	11.04	9.98	17.26	13.68	13.14	10.74
G	4.50	3.87	6.80	5.60	5.02	4.24
K	6.78	7.87	12.53	8.25	12.64	7.87

Values for total anisotropy ΔM (%), relative anisotropy Δm (%), Poisson's ratio (ν), Young's modulus *E* (MPa), shear modulus *G* (MPa) and bulk modulus *K* (MPa).

to ice crystallization inside the pore system. This weight increase shows a similar trend to that observed in samples subjected to free water absorption (Fig. 4). J3 performed best, with the lowest weight increase and smallest fluctuations during the test. At the opposite end were J2 and J6, the stones that absorbed most water during the hydric test. However, although both stones show a slight but

Table 4. *Weight loss (in %) measured in the stones from Bujalance (J1), Baeza (J2 and J3), Sabiote (J4) and Cazorla (J5 and J6) after 15 cycles of the salt crystallization test and 30 cycles of the freeze–thaw test*

	J1	J2	J3	J4	J5	J6
Salt crystallization	23.98	4.65	0.22	3.19	22.67	1.73
Freeze–thaw	0.07	0.18	0.12	0.05	0.13	0.10

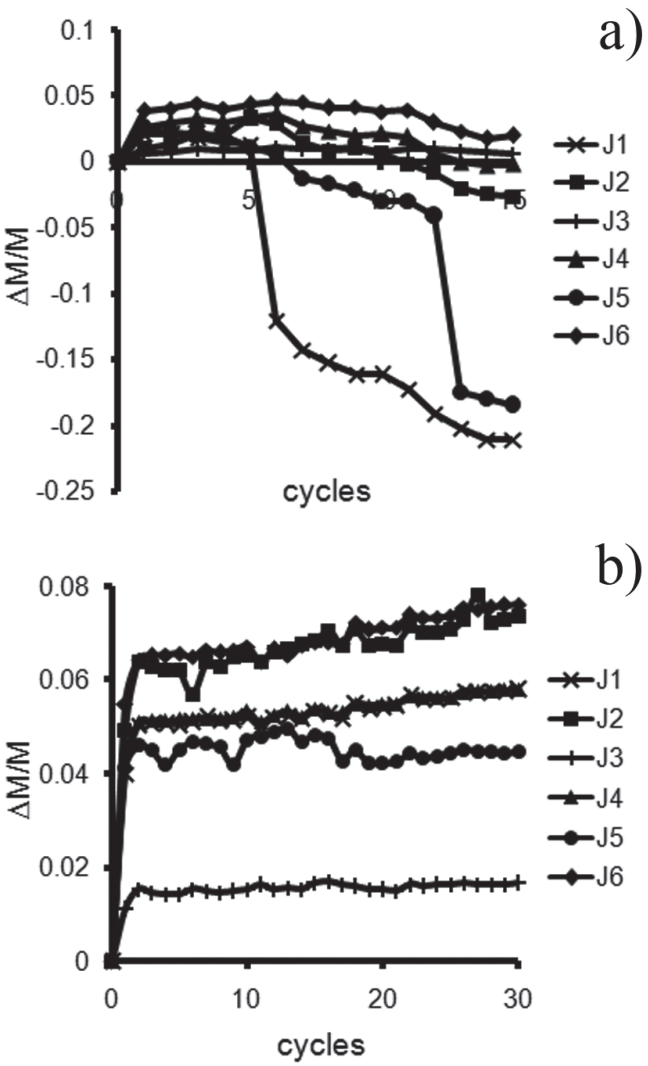

Fig. 5. Weight variation (in %) of the stones from Bujalance (J1), Baeza (J2 and J3), Sabiote (J4) and Cazorla (J5 and J6) submitted to salt crystallization (**a**) and freeze–thaw cycles (**b**).

constant weight increase, the fluctuations in weight were more marked in J2, which showed the highest weight loss (0.18%, Table 4) at the end of the test. The other three stones showed values between these two extremes. J1 and J4 behaved in almost identical fashion (Fig. 5b) with very similar weight losses (0.07% and 0.05%, respectively), whereas J5 showed slightly worse behaviour owing mainly to a greater weight fluctuation. However, at the end of the freeze–thaw test the weight loss was very low in all samples and always less than 0.2%.

As regards changes in colour and lightness, it is interesting to note that all the samples showed a decrease in lightness (L^*), which indicates that they turned slightly darker, and almost all showed an increase in chromaticity (a^* and b^*) after the durability tests (Table 5). This was due to the loss of fragments on the surfaces of

Table 5. *Lightness (L*) and chromatic coordinates (a* and b*) of fresh and decayed stones from Bujalance (J1), Baeza (J2 and J3), Sabiote (J4) and Cazorla (J5 and J6), and colour difference values (ΔE) after salt crystallization and freeze–thaw tests*

	Fresh stone			Salt crystallization				Freeze–thaw			
	*L**	*a**	*b**	*L**	*a**	*b**	*ΔE*	*L**	*a**	*b**	*ΔE*
J1	62.33	2.39	12.83	49.81	5.62	20.43	15.00	57.14	5.68	18.00	8.03
J2	63.43	6.84	21.56	62.23	7.54	25.54	4.21	61.00	10.77	22.15	4.66
J3	62.32	4.63	14.17	59.64	6.24	17.79	4.78	58.01	8.55	16.87	6.42
J4	67.08	2.53	12.38	61.48	4.38	18.20	8.29	67.04	7.77	15.34	6.02
J5	68.22	6.57	19.02	66.09	8.62	25.43	7.06	63.88	12.93	22.46	8.43
J6	64.64	8.11	13.49	54.14	13.37	19.08	13.01	62.62	12.05	15.90	5.04

the stones, which increased their roughness, thus causing a change in colour (and lightness). To be more precise, *a** increased above all when the samples were submitted to the salt crystallization test, whereas *b** increased after the freeze–thaw test. Colour difference (ΔE, Table 5) was moderately perceptible to the naked eye and varied in the range of 4–8 in all samples with the exception of J1 and J6, which underwent significant changes in colour when subjected to the salt crystallization test ($\Delta E > 13$).

Conclusions

The six stones studied in this work show different textures and, in some cases, different mineralogy. These differences result in a variability in the porosity (ranging from *c*. 8 to 21%), the size of pores (the main peak is situated around 10 μm or below 5 μm), the flow of water through the pore system (free water absorption varies from *c*. 2 to 8%), the propagation of ultrasound waves (longitudinal wave velocity ranges from 3500 to 4200 m s^{-1}) and the resistance to decay in accelerated ageing tests (weight loss after the salt crystallization test varies from 0.2 to 24%). These parameters have been useful for evaluating the qualities of these stones and selecting the best ones for use in the construction industry.

Because weathering processes often depend on the circulation of water inside the porous solids (Hall & Hoff 2002), hydric tests are very important for determining stone durability. In these tests, the 'Piedra Viva' stone from Baeza (J3) decayed least, because of its low porosity and low water absorption, even though its pores are poorly interconnected. On the basis of ultrasound, J3 is also the most compact stone. The least anisotropic stones were the reddish calcarenite from Cazorla (J6) and the dolostone from Sabiote (J4).

The decision on which stone to use in a building project depends on the particular type of decay to which the stones are exposed. In addition to the chromatic change that takes place in all stones, J1 (the sandstone from Bujalance) and J5 (one of the two calcarenites from Cazorla) are the most susceptible to salt-induced damage, which means that they should not be used in buildings in which salts are the main source of decay. The other four stones, however, resist well in this situation and can therefore be recommended for use. On the other hand, if cold climatic conditions with temperatures around zero are the main stone decay factor, there is no marked difference: all the stones are suitable, with the 'Piedra Franca' from Baeza (J2) being slightly less durable than the others.

On the basis of the parameters considered in this investigation, the 'Piedra Viva' from Baeza is the one that performs best. The stones with the poorest qualities are the 'Piedra Franca' from Baeza and the reddish calcarenite from Cazorla. The other three stones show intermediate qualities.

Although our results refer to only the stones we studied, the method can be applied to other sedimentary stones to help choose the most suitable materials to use in new buildings and in the restoration of historical monuments.

Acknowledgements. This study was financially supported by Research Group RNM179 of the Junta de Andalucía and by Research Project MAT2008-06799-C03-03. We are grateful to N. Walkington for his assistance in translating the original text.

References

Alcalde, M., Terreros, G.G. & Villegas, R. 1998. Morfología macroscópica de alteración de la piedra de la Catedral de Baeza, Jaén (España). *Materiales de Construcción*, **48**, 27–44.

Alves, C., Figueiredo, C., Maurício, A., Sequeira Braga, M.A. & Aires Barros, L. 2011. Limestones under salt decay tests: Assessment of pore network-dependent durability predictors. *Environmental Earth Sciences*, **63**, 1511–1527.

Anania, L., Badalà, A., *et al*. 2012. The stones in monumental masonry buildings of the 'Val di Noto' area: New data on the relationships between petrographic characters and physical–mechanical properties. *Construction and Building Materials*, **33**, 122–132.

Anonymous. 1988. *Normal 29/88. Misura dell'indice di asciugamento (Drying Index).CNR-ICR*. Rome.

Anonymous. 2001. *EN-12370. Metodi di prova per pietre naturali. Determinazione della resistenza alla cristallizzazione dei sali*. CNR-ICR. Rome.

Anonymous. 2003. *EN-12371. Metodi di prova per pietre naturali. Determinazione della resistenza al gelo*. CNR-ICR. Rome.

Anonymous. 2008. *EN-13755. Metodi di prova per pietre naturali. Determinazione dell'assorbimento d'acqua a pressione atmosferica*. CNR-ICR. Rome.

Anselmetti, F.S., Luthi, S. & Eberli, G.P. 1998. Quantitative characterization of carbonate pore systems by digital image analysis. *AAPG Bulletin*, **82**, 1815–1836.

Ashurst, J. & Dimes, F.G. 1990. *Conservation of Building and Decorative Stone*. Butterworth–Heinemann, Oxford.

ASTM. 1983. *D 2845. Standard Method for Laboratory Determination of Pulse Velocities and Ultrasonic Elastic Constants of Rock*. American Society for Testing and Materials, West Conshohocken, PA.

Charola, A.E. 2004. Stone deterioration in historic buildings and monuments. *In*: Kwiatkowski, D. & Löfvendahl, R. (eds) *Proceedings of the 10th International Congress on Deterioration and Conservation of Stone*. ICOMOS Sweden, Stockholm, 3–14.

Cultrone, G. & Sebastián, E. 2009. Fly ash addition in clayey materials to improve the quality of solid bricks. *Construction and Building Materials*, **23**, 1178–1184.

Cultrone, G., de la Torre, M.J., Sebastián, E. & Cazalla, O. 2003. Evaluation of brick durability using destructive and non-destructive methods (DT and NDT). *Materiales de Construcción*, **53**, 41–59.

Domenico, S.N. 1983. Sandstone and limestone porosity determination from shear and compressional wave velocity. *Bulletin of the Australian Society of Exploration Geophysicists*, **14**, 81–90.

Fort, R. 2008. La piedra natural y el patrimonio construido: Un mismo campo de investigación. *Materiales de Construcción*, **58**, 7–10.

García del Cura, M.A., Benavente, D., Bernabeu, A., Fort, R., La Iglesia, A. & Ordóñez, S. 2005. Las calizas microcristalinas como material de construcción: El caso del Gris Pulpis. *Materiales de Construcción*, **55**, 5–23.

Guydader, J. & Denis, A. 1986. Propagation des ondes dans les roches anisotropes sous contrainte évaluation de la qualité des schistes ardoisiers. *Bulletin of Engineering Geology*, **33**, 49–55.

Hall, C. & Hoff, W.D. 2002. *Water Transport in Brick, Stone and Concrete*. Taylor & Francis, London.

IGME. 1975. *Guía del mapa geológico de Bujalance. Escala 1: 50000*. IGME, Madrid.

Ji, S., Wang, Q. & Salisbury, M.H. 2009. Composition and tectonic evolution of the Chinese continental crust constrained by Poisson's ratio. *Tectonophysics*, **463**, 15–30.

Kirk, R.E. & Othmer, D.F. 2004. *Encyclopedia of Chemical Technology. Vol. 9, Drying*. Wiley, New York, 93–141.

Kühnel, R.A. 2002. Driving forces of rock degradation. *In*: Galán, E. & Zezza, F. (eds) *Protection and Conservation of the Cultural Heritage in the Mediterranean Cities*. Swets & Zeitlinger, Lisse, The Netherlands, 11–17.

Martín, J.D. 2004. *XPowder. A software package for powder X-ray diffraction analysis*. University of Granada, Spain. Legal Deposit GR 1001/04.

Molina, E., Cultrone, G., Sebastián, E., Alonso, F.J., Carrizo, L., Esbert, J. & Buj, O. 2011. The pore system of sedimentary rocks as a key factor in the durability of building materials. *Engineering Journal*, **118**, 110–121.

RILEM. 1980. Recommended tests to measure the deterioration of stone and to assess the effectiveness of treatment methods. *Materials and Structures*, **13**, 175–253.

Ruiz Agudo, E., Rodriguez Navarro, C. & Sebastián Pardo, E. 2006. Sodium sulfate crystallization in presence of phosphonates: Implications in ornamental stone conservation. *Crystal Growth and Design*, **6**, 1575–1583.

Scherer, G.W. 1990. Theory of drying. *Journal of the American Ceramic Society*, **73**, 3–14.

Sebastián, E., Cultrone, G., Benavente, D., Linares Fernandez, L., Elert, K. & Rodriguez Navarro, C. 2008. Swelling damage in clay rich sandstones used in the church of San Mateo in Tarifa (Spain). *Journal of Cultural Heritage*, **9**, 6–76.

Sebastian Pardo, E., Martin Clabo, J. & Zezza, U. 1995. The 'Piedra Dorada' calcarenite in the built heritage of Baeza (Andalusian Province of Jaen, Spain). *Atti Ticinesi di Scienze della Terra*, **38**, 205–213.

Török, A. & Prikryl, R. 2010. Current methods and future trends in testing, durability analyses and provenance studies of natural stones used in historical monuments. *Engineering Geology*, **115**, 139–142.

Veniale, F., Setti, M. & Lodola, S. 2008. Diagnóstico del deterioro de la piedra en el patrimonio construido. Datos y perspectivas. *Materiales de Construcción*, **58**, 11–32.

Whitney, D.L. & Evans, B.W. 2010. Abbreviations for names of rock-forming minerals. *American Mineralogist*, **95**, 185–187.

Winkler, E.M. 1997. *Stone in Architecture: Properties, Durability*. 3rd edn. Springer, Berlin.

Received 6 February 2012; accepted 15 May 2012.